

# North American ice-sheet dynamics and the onset of 100,000-year glacial cycles

R. Bintanja<sup>1,2</sup> & R. S. W. van de Wal<sup>2</sup>

The onset of major glaciations in the Northern Hemisphere about 2.7 million years ago<sup>1</sup> was most probably induced by climate cooling during the late Pliocene epoch<sup>2,3</sup>. These glaciations, during which the Northern Hemisphere ice sheets successively expanded and retreated, are superimposed on this long-term climate trend, and have been linked to variations in the Earth's orbital parameters<sup>4</sup>. One intriguing problem associated with orbitally driven glacial cycles is the transition from 41,000-year to 100,000-year climatic cycles that occurred without an apparent change in insolation forcing<sup>5</sup>. Several hypotheses have been proposed to explain the transition, both including and excluding ice-sheet dynamics<sup>6–10</sup>. Difficulties in finding a conclusive answer to this palaeoclimatic problem are related to the lack of sufficiently long records of ice-sheet volume or sea level. Here we use a comprehensive ice-sheet model and a simple ocean-temperature model<sup>11</sup> to extract three-million-year mutually consistent records of surface air temperature, ice volume and sea level from marine benthic oxygen isotopes<sup>12</sup>. Although these records and their relative phasings are subject to considerable uncertainty owing to limited availability of palaeoclimate constraints, the results suggest that the gradual emergence of the 100,000-year cycles can be attributed to the increased ability of the merged North American ice sheets to survive insolation maxima and reach continental-scale size. The oversized, wet-based ice sheet probably responded to the subsequent insolation maximum by rapid thinning through increased basal-sliding<sup>13,14</sup>, thereby initiating a glacial termination. Based on our assessment of the temporal changes in air temperature and ice volume during individual glacials, we demonstrate the importance of ice dynamics and ice–climate interactions in establishing the 100,000-year glacial cycles, with enhanced North American ice-sheet growth and the subsequent merging of the ice sheets being key elements.

This onset of major glaciations has been inferred primarily from analyses of marine oxygen isotope ratio ( $\delta^{18}\text{O}$ ) records<sup>15</sup>. The glaciations have been confidently linked to variations in the Earth's orbital parameters—that is, precession of the equinoxes (with periods of 19,000 and 23,000 years; 19 and 23 kyr), axial obliquity (41 kyr) and orbital eccentricity (100 kyr)<sup>4</sup>. However, difficulties associated with the theory of orbitally driven glacial cycles remain. One of the more intriguing problems relates to the observation that marine  $\delta^{18}\text{O}$  varied mainly at obliquity timescales before  $\sim 1$  Myr ago<sup>16</sup> and at 100-kyr timescales thereafter. This transition from 41-kyr to 100-kyr climatic cycles is generally known as the mid-Pleistocene transition (MPT), and occurred without an apparent change in insolation forcing. Numerous explanations have been proposed for this change, such as a nonlinear ice-sheet response to a long-term cooling trend<sup>6</sup>, spatial and temporal changes in ice-sheet substratum<sup>7</sup>, sea-ice effects on ablation and accumulation<sup>8</sup>, orbital-inclination forcing induced

by extraterrestrial dust<sup>9</sup>, and a change in the margin of the Antarctic ice sheet from land-based to marine-based<sup>10</sup>.

The main difficulty in finding conclusive answers to this long-standing palaeoclimatic question is that sufficiently long records of ice-sheet volume or sea level are currently unavailable. Hence, existing hypotheses are mostly based on benthic  $\delta^{18}\text{O}$  records. However, these are influenced not only by the mean oceanic  $\delta^{18}\text{O}$  (governed by Northern Hemisphere ice-sheet storage) but also by local deep-water temperature<sup>17</sup>, and marine  $\delta^{18}\text{O}$  records may therefore be poor indicators of ice-sheet fluctuations in terms of their volume<sup>11</sup> and phase lag owing to the temperature overprint<sup>18–20</sup>.

We have applied a recently developed model-based method<sup>11</sup> to separate these two components, which involves an inverse technique in conjunction with an ice-sheet model coupled to a simple deep-water temperature model (Supplementary Information and Methods). Using the LR04 stack marine  $\delta^{18}\text{O}$  record<sup>12</sup>, we have reconstructed mutually consistent 3-Myr time series of surface air temperature (continental and annual mean between 40° and 80° N), ice-sheet volume and sea level. We have estimated the phasing between them to deduce causes and effects, and infer how the climate variables and phasings have changed over the MPT. These reconstructions are subject to considerable uncertainty<sup>11</sup>, in particular before 0.4 Myr ago, which is due mainly to limited palaeoclimatic constraints (Supplementary Information) and to the simplicity of the ocean-temperature model (and other assumptions<sup>11</sup>).

The reconstructed marine isotope signal increased steadily over the past 3 Myr (Fig. 1a), indicative of both climatic cooling (Fig. 1b) and growing ice sheets (Fig. 1c) (Supplementary Data). Its amplitude (reflecting the contrast between interglacial and glacial states) also increased with time, with noticeable changes occurring around 2.7 Myr ago<sup>21</sup> indicating the onset of Northern Hemisphere glaciation (Fig. 1c), and again around 1 Myr ago (MPT). The inferred overall 3-Myr cooling trend is generally consistent with the gradual cooling of alkenone-derived equatorial sea surface temperature from deep-sea sediment cores<sup>3</sup>, although our mid-latitude/subarctic cooling is stronger, most probably implying an increase in meridional temperature gradient over the 3-Myr period. Our reconstructed deep-sea cooling of about 2–2.5 °C agrees with Mg/Ca deep-sea temperature estimates<sup>2</sup> (Supplementary Information).

According to our calculations, the inception of the Northern Hemisphere ice sheets at about 2.7 Myr ago may be linked to air temperatures dropping below  $-5$  °C (relative to the present), with summer temperatures over inception-sensitive regions being the critical factor<sup>22</sup>. The modelled timing of Northern Hemisphere inception coincides with the first occurrence of ice-rafted debris in the North Atlantic<sup>23</sup>, which indicates calving ice sheets bordering the ocean. The amplitude of the temperature fluctuations hardly increased (Fig. 1b) during this inception period, suggesting that the emerging Northern

<sup>1</sup>Royal Netherlands Meteorological Institute (KNMI), Wilhelminalaan 10, 3732 GK De Bilt, The Netherlands. <sup>2</sup>Institute for Marine and Atmospheric Research Utrecht (IMAU), Utrecht University, Princetonplein 5, 3584 CC Utrecht, The Netherlands.

Hemisphere ice sheets accounted for the enhanced  $\delta^{18}\text{O}$  variability around 2.7 Myr ago.

Following Northern Hemisphere glacial inception, a more gradual cooling facilitated steady ice-sheet expansion over the past 2.5 Myr (in the long-term average; thick lines in Fig. 1a, b). Before the MPT, the Eurasian (EAS) ice sheets contributed most to the total Northern Hemisphere ice volume; then, with the appearance of 100-kyr glacials, the North American (NAM) ice sheets took over. According to our model calculations, the EAS and NAM ice sheets on average stored 19.0 and 15.8 m sea level equivalent (m.s.l.e.), respectively, between 1 and 2 Myr ago, and 25.9 and 29.6 m.s.l.e. in the past 1 Myr, suggesting that the MPT somehow involved a change in EAS and NAM ice-sheet characteristics. With the emergence of the 100-kyr cycles during the MPT, the  $\delta^{18}\text{O}$  signal again exhibits a marked increase in amplitude. Our results suggest that this can be attributed mainly to an increase in the glacial–interglacial range of ice volume and global sea level (Fig. 1c), as air temperature fluctuations exhibit only a modest increase in amplitude.

Most theories about the causes and origin of ice ages (glacials), including those involving the MPT, rely heavily on assumptions regarding the phasing of temperature, ice volume and  $\delta^{18}\text{O}$  fluctuations relative to each other and to insolation components<sup>19,21</sup>. Here we estimate these phasings using Blackman–Tukey cross-spectral analysis to determine the phase and coherence spectra relative to

the 21 June insolation at 65° N. The results suggest that temperature exhibited a relatively small lag relative to insolation, which increased from 1.5 kyr at 2.5 Myr ago to 4.5 kyr at present (Fig. 2a), presumably caused by the thermal effects of expanding ice sheets. Because temperature and  $\text{CO}_2$  most probably varied roughly in phase<sup>19</sup>, our results indicate that obliquity forced Northern Hemisphere temperatures—most probably through mechanisms associated with the global carbon cycle—then drove the Northern Hemisphere ice sheets. Global ice volume lagged behind insolation and temperature by several millennia, with the EAS ice sheets exhibiting the slowest response because of colder and drier ambient conditions.

The average lag of ice volume behind surface air temperature decreased from about 6 kyr at 2.5 Myr ago to slightly more than 3 kyr at present (Fig. 2a), with the strongest decrease occurring after the MPT. According to our calculations, the Northern Hemisphere needed to cool about 5 °C before ice-sheet inception occurred. Also, ice sheets cannot expand faster than the rate at which mass is gained through snow accumulation. Both factors contribute to ice volume lagging temperature by 5–7 kyr during inception stages, both for 41-kyr and 100-kyr glaciations, indicating that ice-sheet growth merely followed the temperature signal. The only exception to ice volume lagging air temperature involves 100-kyr deglaciations; the associated lag dropped to about zero during the MPT (Fig. 2b). This suggests the existence of two ‘regimes’: before the MPT, deglaciations of small ice

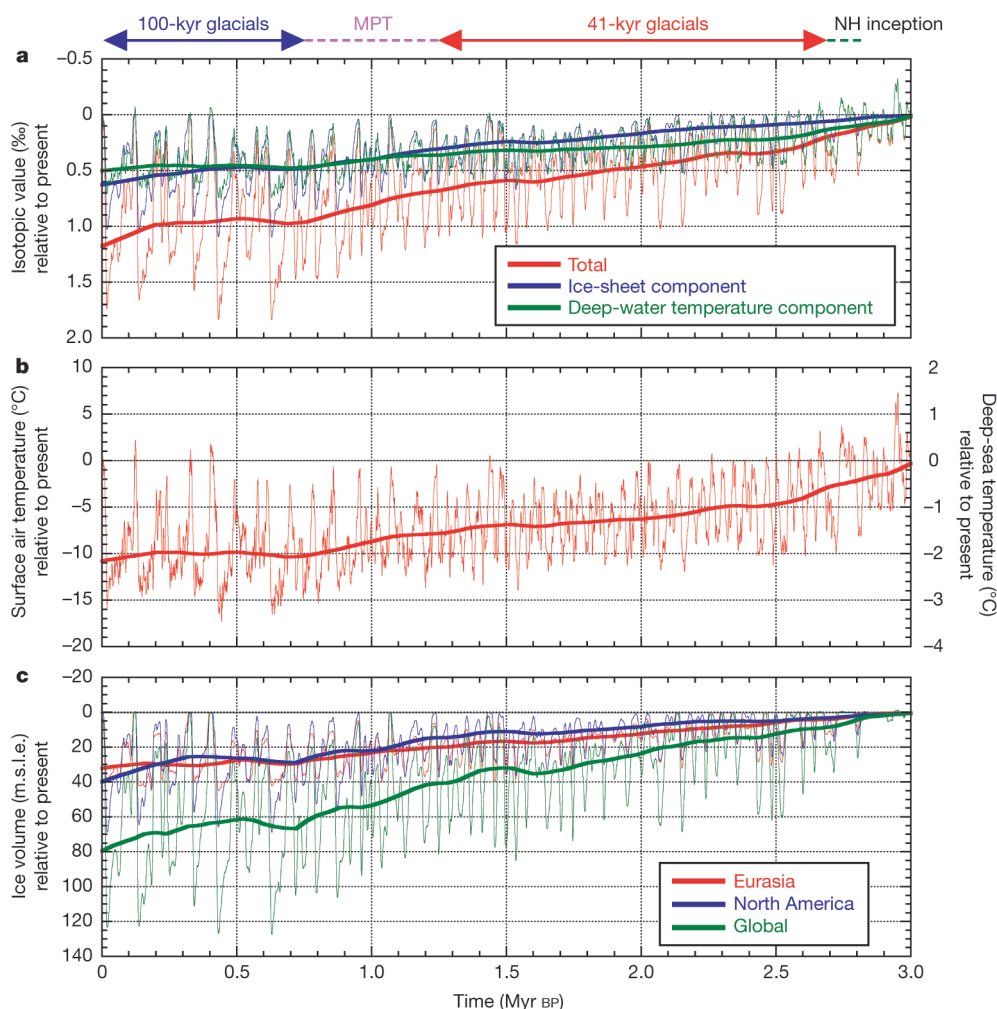


**Figure 1 | Three-million-year time series of marine oxygen isotope values, subarctic surface air temperature and ice volume.** Thick lines represent 400-kyr running means. **a**, Input marine oxygen isotope ( $\delta^{18}\text{O}$ ) stack record<sup>12</sup> with the present-day value of 3.22‰ subtracted (red), and the reconstructed ice-sheet (blue) and deep-water temperature (green) components. **b**, Reconstructed surface air temperature (annual average

Northern Hemisphere continents between 40° and 80° N) and deep-ocean temperature. **c**, Reconstructed sea level or global ice volume (green), and the Eurasian (red) and North American (blue) contributions. Coloured lines/arrows along top represent various stages of glaciation. MPT, mid-Pleistocene transition; NH, Northern Hemisphere; BP, before present; m.s.l.e., m sea level equivalent.

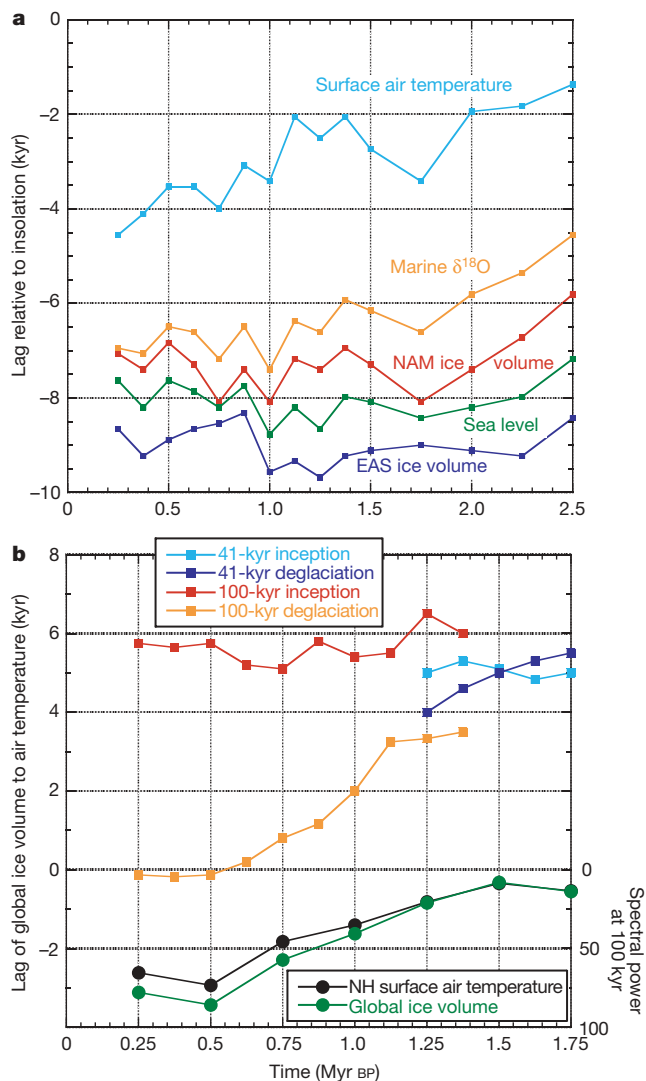


**Figure 2 | Phase lags of input/reconstructed variables, as evaluated using Blackman–Tukey cross-spectral analysis with 30% lags.** Data points represent 500-kyr windows. **a**, Phase lag at 41 kyr (obliquity) of Northern Hemisphere surface air temperature, Eurasian (EAS) ice volume, North American (NAM) ice volume, global sea level or total ice volume, and total marine oxygen isotope ( $\delta^{18}\text{O}$ ) value, relative to insolation ( $65^\circ\text{N}$ , 21 June). For the obliquity spectral component, the coherence is always above the 95% confidence level for all variables considered, whereas the reconstructed records are generally incoherent with respect to the precession component and also to the eccentricity components (before 1.2 Myr ago). As the tuning of the LR04 stack emphasizes obliquity, the associated lag is primarily determined by the assumed time constant of the simple ice model that was used for tuning<sup>12</sup>. The lag of  $\delta^{18}\text{O}$  relative to insolation increased between 2.5 and 1.5 Myr ago, after which it remained largely constant, as this was prescribed as such in the tuning of the LR04 stack<sup>12</sup>. Lags and leads of all other variables relative to  $\delta^{18}\text{O}$  are independent of this tuning procedure, but are most probably associated with considerable uncertainty owing to the limited availability of palaeoclimate constraints and to the simplicity of mainly the ocean model<sup>11</sup>. **b**, Upper four curves (left axis) show phase lag of global ice volume to Northern Hemisphere surface air temperature for 41-kyr inception and deglaciation stages (light and dark blue) and for 100-kyr inception and deglaciation stages (red and orange). Lower two curves (right axis) show spectral power of 100-kyr Northern Hemisphere surface air temperature (black) and global sea level or ice volume (green) variations.

sheets linearly followed temperature, whereas after the MPT the huge ice sheets were actively involved in the rapid, nonlinear deglaciations to terminate the 100-kyr glacials. Even though they were ultimately triggered by insolation, inceptions were probably governed by non-ice-sheet climate feedbacks to decrease temperature below the threshold of ice-sheet inception, whereas glacial terminations presumably actively involved the rapid break-up of vulnerable large ice sheets<sup>13,24</sup>, both agreeing with phase relationships over the last 360 kyr derived from Antarctic ice cores<sup>25</sup>.

We note that the resulting phasings of reconstructed variables relative to insolation are largely determined by the choices made to construct the age model of LR04 (which determines the phase between  $\delta^{18}\text{O}$  and insolation). However, the 1.5–4.5-kyr lag between reconstructed air temperature and insolation (Fig. 2a) agrees well with the response timescale of the important feedback mechanisms in the climate system (ocean, carbon cycle, ice sheets), suggesting that the phasings assumed in LR04 are realistic. Also, the reconstructed

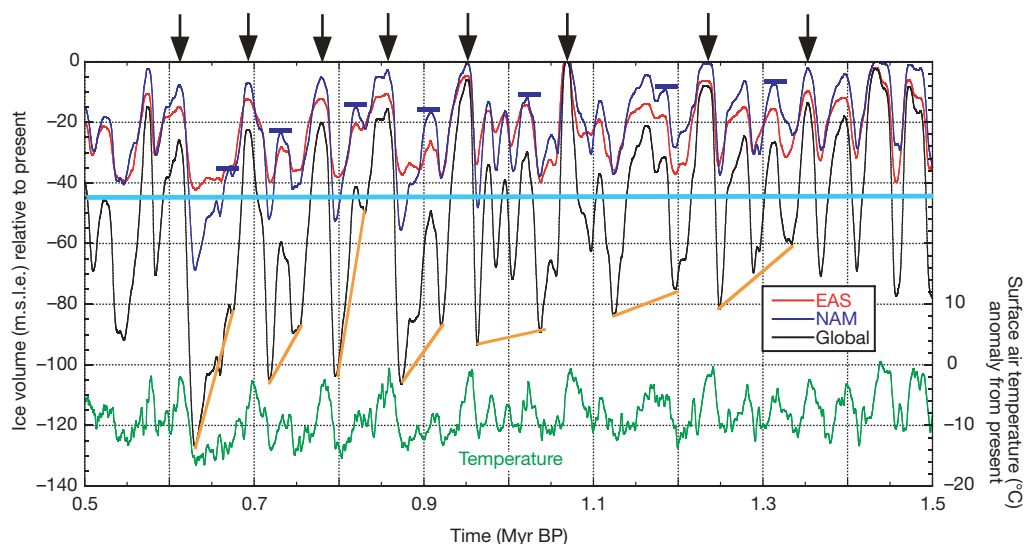


**Figure 3 | Time series of ice volume and Northern Hemisphere subarctic surface air temperature between 1.5 and 0.5 Myr ago, across the MPT.** Left axis, ice volume; global, Eurasian (EAS) and North American (NAM) contributions are shown as black, red and dark blue curves, respectively. Right axis, Northern Hemisphere subarctic surface air temperature (green curve). Vertical black arrows depict inferred 100-kyr interglacials.

Horizontal dark blue bars represent the first NAM ice volume minimum following a 100-kyr interglacial. The horizontal light blue line represents the 45 m.s.l.e. level beyond which the Cordilleran and Laurentide ice sheets in North America merged (Supplementary Information), which occurred only after 1 Myr ago. Orange lines connect maxima in global ice volume within a single 100-kyr glacial, highlighting increasing ice volumes during a glacial.



lags to insolation vary in time in a manner not prescribed by LR04. These and other considerations (see Supplementary Information) indicate that our analysis provides a picture of the phasings between climate variables and insolation that is consistent overall.

Our results support other analyses in showing that the MPT represents a fairly gradual increase in 100-kyr power (Fig. 2b) from (roughly) 1.4 to 0.6 Myr ago<sup>5,13,26</sup>. An important feature is the increased inability of the system to reach full interglacial levels at the obliquity and precession timescales (Fig. 3), in particular in North America where continuing cooling enabled ice sheets to overcome insolation maxima at ever greater volumes<sup>6,24</sup>. This produced further expansion and eventual merging (at about 45 m.s.l.e.) of the Cordilleran and the Laurentide ice sheets. In Eurasia, the post-MPT ice volume was still limited to about 40 m.s.l.e., presumably because the Atlantic Ocean in the west and the dry and cold Siberian plains to the east prevented further expansion of the Fennoscandian ice sheet<sup>11</sup>.

The appearance of full-grown, merged ice sheets in North America coincided with the deglaciation lag between surface air temperature and ice volume being reduced to about zero (Fig. 2b), suggesting a leading role for the NAM ice sheets in glacial terminations. We argue that this large NAM ice volume initiated rapid deglaciations involving large ice cap instabilities<sup>17,27</sup>, because similar insolation maxima apparently failed to trigger deglaciations of less extensive ice sheets. Thick, wet-based ice sheets are particularly sensitive to climate warming<sup>13,14</sup>. Hence, once the NAM ice sheets reached a certain threshold size (about 70 m.s.l.e.) during the post-MPT glacials, the following insolation maximum and associated air temperature peak triggered a rapid thinning of the ice sheet through increased sliding rates<sup>28</sup>, presumably via fast-flowing ice streams and possibly enhanced by ablation, sea level and ocean circulation feedbacks<sup>6,10,29</sup> (Supplementary Information).

Even though our 3-Myr reconstructions of temperature, ice volume and sea level should be considered first-order estimates—mainly owing to the limited availability of constraining palaeoclimate data—they nevertheless suggest that differences between the NAM and EAS ice sheets were central to the gradual emergence of the 100-kyr glacials between 1.4 and 0.6 Myr ago. Whereas the dry and sluggish EAS ice sheets dominated before the MPT, increased climate cooling enabled the NAM ice sheets to expand and eventually combine into one large ice sheet that ultimately became unstable, triggering rapid glacial terminations. The duration of the post-MPT glacials of 80–120 kyr (2–3 obliquity cycles) was essentially governed by the rate at which the NAM ice sheets expanded. According to this hypothesis, specific ice dynamics and ice–climate interactions related to the North American ice sheets played a crucial role in establishing the 100-kyr glacial cycles.

## METHODS SUMMARY

The key to separating the LR04 stack marine  $\delta^{18}\text{O}$  record<sup>12</sup> into actual climate data is the observation that the two main components affecting the marine  $\delta^{18}\text{O}$  value (storage in ice sheets and deep-water temperature) both rely heavily on surface air temperature (with regard to long-term changes). By using models that describe these relationships (an elaborate ice-sheet model to link air temperature to ice volume and ice  $\delta^{18}\text{O}$  storage, and a simple ocean-temperature model to couple deep-water temperature to surface air temperature) in conjunction with an inverse methodology, we were able to quantify the two components<sup>11</sup> for the 3-Myr LR04 stack marine  $\delta^{18}\text{O}$  record. In the process, 3-Myr-long mutually consistent records of atmospheric temperature, ice volume and global sea level were reconstructed. Using Blackman–Tukey cross-spectral analysis, we estimated the phasings between these climate records in order to assess causes and effects during glacial fluctuation, mainly for inception and termination stages. Even though the Blackman–Tukey method has its drawbacks in terms of accuracy, we decided to use it to compare our phasings with those of LR04 (where it was also used). The main problem with new long records such as those presented here is to find sufficiently long and independent records for validation. A comparison between our reconstructed records and existing independent proxy records is presented in the Supplementary Information.

Received 13 April; accepted 27 May 2008.

1. Raymo, M. E. The initiation of Northern Hemisphere glaciation. *Annu. Rev. Earth Planet. Sci.* **22**, 353–383 (1994).
2. Lear, C. H., Elderfield, H. & Wilson, P. A. Cenozoic deep-sea temperatures and global ice volumes from Mg/Ca in benthic foraminiferal calcite. *Science* **287**, 269–272 (2000).
3. Lawrence, K. T., Zhonghui, L. & Herbert, T. D. Evolution of the eastern tropical Pacific through Plio-Pleistocene glaciation. *Science* **312**, 79–83 (2006).
4. Hays, J. D., Imbrie, J. & Shackleton, N. J. Variation in the Earth's orbit: Pacemaker of the ice ages. *Science* **194**, 1121–1132 (1976).
5. Clark, P. U. *et al.* The middle Pleistocene transition: Characteristics, mechanisms, and implication for long-term changes in atmospheric  $\text{pCO}_2$ . *Quat. Sci. Rev.* **25**, 3150–3184 (2006).
6. Berger, A., Li, X. S. & Loutre, M. F. Modelling northern hemisphere ice volume over the last 3 Ma. *Quat. Sci. Rev.* **18**, 1–11 (1999).
7. Clark, P. U. & Pollard, D. Origin of the Middle Pleistocene transition by ice sheet erosion of regolith. *Paleoceanography* **13**, 1–9 (1998).
8. Tziperman, E. & Gildor, H. On the mid-Pleistocene transition to 100-kyr glacial cycles and the asymmetry between glaciation and deglaciation times. *Paleoceanography* **18**, 1001, doi:10.1029/2001PA000627 (2003).
9. Muller, R. A. & MacDonald, G. J. Glacial cycles and orbital inclination. *Nature* **377**, 107–108 (1995).
10. Raymo, M. E., Lisiecki, L. E. & Nisancioglu, K. H. Plio-Pleistocene ice volume, Antarctic climate, and the global  $\delta^{18}\text{O}$  record. *Science* **313**, 492–495 (2006).
11. Bintanja, R., van de Wal, R. S. W. & Oerlemans, J. Modelled atmospheric temperatures and global sea level over the past million years. *Nature* **437**, 125–128 (2005).
12. Lisiecki, L. E. & Raymo, M. E. A Pliocene-Pleistocene stack of 57 globally distributed benthic  $\delta^{18}\text{O}$  records. *Paleoceanography* **20**, doi:10.1029/2004PA001071 (2005).
13. Clark, P. U., Alley, R. B. & Pollard, D. Northern Hemisphere ice-sheet influences on global climate change. *Science* **286**, 1104–1111 (1999).
14. Marshall, S. J. & Clark, P. U. Basal temperature evolution of North American ice sheets and implications for the 100-kyr cycle. *Geophys. Res. Lett.* **29**, doi:10.1029/2002GL015192 (2002).
15. Lisiecki, L. E. & Raymo, M. E. Plio-Pleistocene climate revolution: Trend and transitions in glacial cycles. *Quat. Sci. Rev.* **26**, 56–69 (2007).
16. Raymo, M. E. & Nisancioglu, K. H. The 41 kyr world: Milankovitch's other unsolved mystery. *Paleoceanography* **18**, 1011, doi:10.1029/2002PA000791 (2003).
17. Imbrie, J. *et al.* in *Milankovitch and Climate* (ed. Berger, A. L.) 269–305 (Reidel, Dordrecht, 1984).
18. Maslin, M. A., Li, X. S., Loutre, M. F. & Berger, A. The contribution of orbital forcing to the progressive intensification of northern hemisphere glaciation. *Quat. Sci. Res.* **17**, 411–426 (1998).
19. Ruddiman, W. F. Orbital insolation, ice volume and greenhouse gases. *Quat. Sci. Rev.* **22**, 1597–1629 (2003).
20. Shackleton, N. J. The 100,000-year ice-age cycle identified and found to lag temperature, carbon dioxide, and orbital eccentricity. *Science* **289**, 1897–1902 (2000).
21. Maslin, M. A. & Ridgeway, A. J. in *Early-Middle Pleistocene Transitions: The Land-Ocean Evidence* (eds Head, M. J. & Gibbard, P. L.) 19–34 (GSL Special Publication Vol. 247, Geological Society, London, 2006).
22. Valdes, P. & Glover, R. W. Modelling the climate response to orbital forcing. *Phil. Trans. R. Soc. Lond. A* **357**, 1873–1890 (1999).
23. Shackleton, N. J. *et al.* Oxygen isotope calibration of the onset of ice-rafting and history of glaciation in the North Atlantic region. *Nature* **307**, 620–623 (1984).
24. Raymo, M. E. The timing of major climate terminations. *Paleoceanography* **12**, 577–585 (1997).
25. Kawamura, K. *et al.* Northern Hemisphere forcing of climatic cycles in Antarctica over the past 360,000 years. *Nature* **448**, 912–916 (2007).
26. Huybers, P. Glacial variability over the last two million years: An extended depth-derived age model, continuous obliquity pacing, and the Pleistocene progression. *Quat. Sci. Rev.* **26**, 37–55 (2007).
27. Weertman, J. Stability of the junction between an ice sheet and an ice shelf. *J. Glaciol.* **13**, 3–11 (1974).
28. Parrenin, F. & Paillard, D. Amplitude and phase of glacial cycles from a conceptual model. *Earth Planet. Sci. Lett.* **214**, 243–250 (2003).
29. Alley, R. B. & Clark, P. U. The deglaciation of the Northern Hemisphere: A global perspective. *Annu. Rev. Earth Planet. Sci.* **27**, 149–182 (1999).

**Supplementary Information** is linked to the online version of the paper at [www.nature.com/nature](http://www.nature.com/nature).

**Acknowledgements** Financial support to R.B. was provided by the Netherlands Organisation of Scientific Research (NWO), in the framework of the SPINOZA award of J. Oerlemans, and through the EU programme Quantify. This work was initiated during the start-up phase of the Utrecht Centre for Geosciences (UCG) programme. We thank W. Greuell, D. Lea, L. Lourens, M. Siddall and N. Weber for remarks on earlier versions of the paper.

**Author Information** Reprints and permissions information is available at [www.nature.com/reprints](http://www.nature.com/reprints). Correspondence and requests for materials should be addressed to R.B. (bintanja@knmi.nl).